fibers

MDPI

Article

Elaboration of High Permeable Macrovoid Free Polysulfone Hollow Fiber Membranes for Air Separation

George Dibrov [1,*], Mikhail Ivanov [1], Mikhail Semyashkin [1], Vladislav Sudin [2], Nikita Fateev [1] and George Kagramanov [1]

[1] D.Mendeleev University of Chemical Technology of Russia, 125047 Moscow, Russia; mihail-ivan0v@yandex.ru (M.I.); mixailsem@rambler.ru (M.S.); n.fateev@lenta.ru (N.F.); kadri@muctr.ru (G.K.)

[2] Baikov Institute of Metallurgy and Materials Science, Russian Academy of Sciences, 119991 Moscow, Russia; sudin.vlad@gmail.com

* Correspondence: george.dibrov@gmail.com; Tel.: +7-915-2119477

Received: 31 March 2019; Accepted: 13 May 2019; Published: 15 May 2019

Abstract: In this work, polysulfone hollow fibers with oxygen permeance 70 L (STP)/(m^2·h·bar) and selectivity $\alpha(O_2/N_2)$ = 6 were obtained. A decrease in the dope solution temperature allowed to diminish macrovoids due to the increase of the dope viscosity from 15.5 Pa·s at 62 °C to 35 Pa·s at 25 °C. To reduce the fiber diameter, thereby increasing the packing density, they were spun at high linear velocities. A hollow fiber membrane element was produced with effective membrane area 2.75 m^2 and packing density 53%. Its air separation performance was evaluated to bridge laboratory studies and practical application.

Keywords: hollow fiber membranes; polysulfone; air; gas separation; nitrogen

1. Introduction

Membrane air separation is now widely accepted as an economic process to produce membrane purity streams containing up to 99.5% nitrogen or 30–50% oxygen [1]. The companies, such as Ube, Air Liquid, Evonik, Generon, and Air Products, are the biggest manufactures of membrane elements (ME) based on asymmetric hollow fiber for this task. Despite the maturity in this area, the most important gas separation characteristics of commercial membranes—permeance and selectivity—are classified.

Permeance (P/l) defines the required membrane area, that is, the size and the number of membrane elements and hence, a substantial portion of the capital cost [2]. This parameter is calculated using a formula:

$$\frac{P}{l} = \frac{V}{\tau S \Delta p}, \quad (1)$$

where P–permeability, l–selective layer thickness, V/τ–volumetric flow rate, S–membrane area, Δp–transmembrane pressure. Units for permeance are: L (STP)/(m^2·h·bar) = 0.3703 GPU = $1.239 \cdot 10^{-10}$ mol/(m^2·s·Pa). Dimensionless membrane selectivity is calculated as a ratio of permeances of fast permeating species (A) relative to slow permeating species (B):

$$\alpha(A/B) = \frac{P_A/l}{P_B/l}. \quad (2)$$

Catalogs can be received on the websites or on demand from major producers of air separation MEs, which can be used to retrieve selectivity. Due to the fact that the membrane area is concealed, a precise calculation of permeance is impossible.

Commercially available membrane systems for air separation are usually fed from the bore side. In such a configuration, the distribution of feed on the membrane surface is evener, which is required for an efficient operation [1]. Usually, the selective layer is positioned on the shell side. Operating transmembrane pressure usually ranges from 5–16 bar [3]. In bore-side feed, the gas permeance slightly increases with pressure, while in shell-side feed, the permeance decreases with pressure [4]. One of the polymers utilized for commercial air separation is polysulfone.

Since the first application of polysulfone (PSf or PSU) hollow fibers in the early 1980s [5] for the commercial gas separation by Monsanto (later Air Products), this polymer has gained a firm position between most widely used membrane materials. Polysulfone was also the object of intensive academic studies. For example, it was employed to produce hollow fibers for ultrafiltration [6–9], membrane contactors [10–16], and gas separation [17–21].

First generation gas separation PSf hollow fibers were spun from formylpiperidine/formamide with the observable selective layer thickness of 500–700 nm [20]. Lewis acid: base complexes were used to produce second-generation PSf membranes [21]. Hollow fiber membranes were obtained with O_2 permeance 116 L (STP)/(m^2·h·bar) and selectivity $\alpha(O_2/N_2)$ = 5 at 50 °C. Later, N-methyl-2-pyrrolidone (NMP)/water and NMP/ethanol were used to yield silicone-coated hollow fibers which exhibited O_2 permeance 55–80 L (STP)/(m^2·h·bar) and O_2/N_2 selectivity 5–6.5 [19]. The effective selective layer thickness estimated by gas permeation was about 36–50 nm.

Polysulfone hollow fibers with improved selectivity were obtained by replacing NMP as the solvent by tetrahydrofuran (THF)/NMP mixture [17]. THF was evaporated from the membrane surface during casting. Therefore, a thicker skin-layer was produced, macromolecules were better oriented, and few pores or defects were generated.

Previously reported gas separation membrane from polysulfone had either low permeance [20] or macrovoids [17,19], large pores which jeopardize the mechanical integrity of a hollow fiber. The aim of this work was to obtain high permeable, defect-free, and macrovoid free hollow fibers from polysulfone for the separation of air. In order to fit with the commercial state of the art, hollow fibers were spun at high linear velocities to reduce the fiber diameter and, thereby, increase the packing density (fraction of the cross-section area of all fibers per cross-section area of the module). The membrane element from these fibers was studied in the process of nitrogen generation.

2. Materials and Methods

2.1. Materials

Polysulfone Ultrason S6010 natural was provided by BASF (Germany). Nitrogen (99.995% vol.) and oxygen (99.999% vol.) were supplied by Moscow Gas Processing Plant (MGPZ). The following reagents were used in this work: dimethylacetamide (DMAc), tetrahydrofuran (THF), isopropanol (IPA), hexane. Reagents were purchased from Khimmed and were of analytical grade. Ethanol (EtOH, 95%) was purchased from Spirtmed. Reverse-osmosis water with a specific conductivity not exceeding 0.06 µS/cm was obtained on-site. Sylgard 184 (polydymethylsiloxane (PDMS)) was produced by Dow Corning.

2.2. Asymmetric Hollow Fiber Spinning and Characterization

Asymmetric hollow fiber membranes were made using the "dry–wet" spinning technique. For asymmetric hollow fibers to possess good mechanical properties, the polymer content in the dope solution was chosen to be 28% wt. The dope (polymeric solution) contained DMAc as a good solvent and ethanol as a non-solvent. The concentration of THF as a moderate solvent was chosen as 15 % wt. because of the positive results described in previous studies [17,22]. THF has high volatility and improves selective layer formation. The dope composition was determined using the cloud-point technique, by picking the highest possible concentration of ethanol in a solution containing the PSf, DMAc, and THF before the turbidity emerged (i.e., phase separation occurred).

The derived solution composition was 28% wt. of polymer, 45% wt. of DMAc, 15% wt. of THF, and 12% wt. of ethanol. PSf was added into DMAc at 50 °C, at constant stirring. Afterward, THF and ethanol were added. To prevent the evaporation of volatile solvents (THF and ethanol) during mixing, a stirrer bearing with a dynamic double seal was employed. To control the loss of solvents, the total weight of the solution was measured. Afterward, dope was kept undisturbed at 50 °C overnight for degassing. The viscosity of the dope solution was determined using a falling ball viscometer.

The schematic of the setup is described in detail in [2,22–24]. The dope was placed in a sealed tank, equipped with a water jacket, and either cooled down to 25 °C or warmed up till 62 °C. Spinneret with the dope orifice outer diameter (OD) of 0.5 mm and the inner diameter (ID) of 0.23 mm was used (Figure 1). The spinneret consisted of four main parts made from brass: housing, internal coagulant supply plug with a screw, internal coagulant connection pipe, and a screw cap. Dope solution and internal coagulant compartments were separated by Teflon gaskets. The flow rate of the dope solution was continuously kept at 0.8 g/min. Water at 50 °C was used as an internal coagulant with a persistent flow rate of 0.8 g/min, while the water at room temperature was used in coagulation and washing baths.

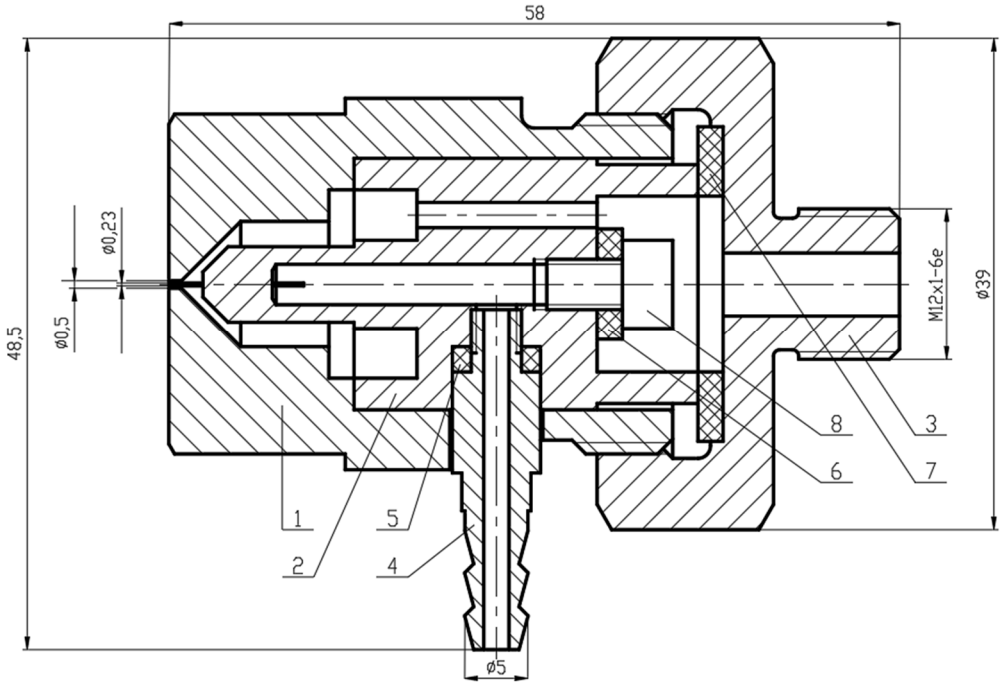

Figure 1. The spinneret design. 1, housing; 2, internal coagulant supply plug; 3, screw cap; 4, internal coagulant connection pipe; 5–7, Teflon gasket; 8, screw.

Resulting hollow fibers were placed in water for 48 h to remove the residual solvent. The sequential solvent substitutions were employed to prevent the pore collapse: the membrane was placed for 48 h in IPA, then for 8 h in hexane, and finally dried in a vacuum (76 mmHg) for 12 h. Furthermore, it was revealed that conditioning in IPA for 48 h increased the permeance of hollow fibers without diminishing their selectivity.

To plug the defects in thin dense skin-layer, hollow fibers were treated with 1% wt. PDMS solution in hexane. New rubbery polymer materials for gas separation applicable for this task were reported in previous studies [25,26].

Afterward, membranes were dried in ambient air for 1–2 h and annealed in air at 60 °C for 3–4 h. This was performed to fully cross-link PDMS and stabilize geometrical and separation characteristics of the membrane because physical aging is known to occur faster at higher temperatures [27].

Pure oxygen and nitrogen permeances were determined using a constant pressure variable volume technique, using the setup shown in Figure 2. Fibers were glued with a polyester inside a 6 mm John

Guest transparent LDPE tube. Bore-side feed was applied at pressure difference Δp = 5 bar and ambient temperature T = 22 ± 2 °C. At least 10 fibers from each batch were measured. Error in gas permeance measurement was not greater than 7%, and for the selectivity calculation, did not exceed 14%.

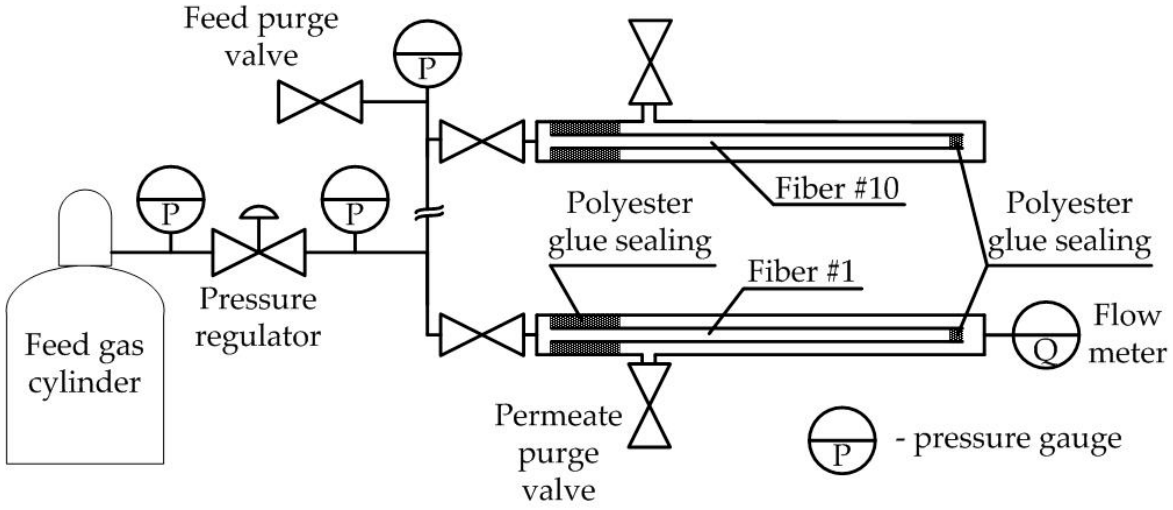

Figure 2. The setup of the pure gas permeance measurement.

To determine the ID and OD of each membrane Levenhuk 40 L NG microscope with a C310 NG, 3M digital camera was employed. Samples were kept for 0.5–1 h in ethanol and subsequently fractured in liquid nitrogen. Deviation in fiber diameters from one batch did not surpass 7%.

Cross-sections of freeze-fractured asymmetric hollow fibers were examined by scanning electron microscopy (SEM). A high-resolution scanning electron microscope Supra 50 VP LEO (Carl Zeiss SMT Ltd., Oberkochen, Germany) was employed at an accelerating voltage of 4.5 kV and an aperture of 30 μm.

2.3. Membrane Element Preparation

Membrane element (ME) was produced in a transparent polyvinyl chloride tube with ID = 28.2 mm, OD = 32 mm. The ME was constructed with the bore side feed of the device and was operated in a countercurrent mode (Figure 3).

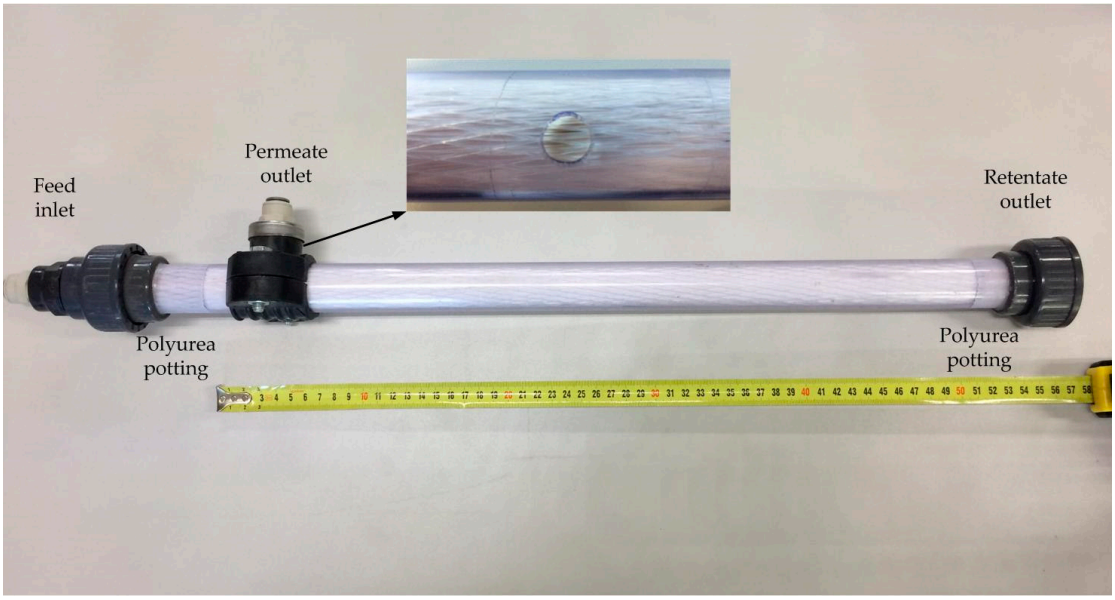

Figure 3. The photograph of the membrane element.

To this effect, a bundle from 8000 untreated with PDMS fibers was placed inside a netlike flexible sleeve and fixed inside the tube. The adhesive was applied to each bundle end to seal membranes and prevent the penetration of polyurea resin to the fiber lumens.

Caps were attached to each end of the tube by a polyester thermal glue gun. Caps were connected through holes by 4 mm hose with bottles, which were also attached to the assembly. Bottles were filled with polyurea resin, and the assembly was centrifuged at 300 rpm for 8 h to better dispense the highly viscous polyurea resin between membranes and prevent the capillary uprise.

Afterward, caps with bottles were detached, each end was heated up to 60 °C to soften the polyurea resin and cut with a sharp blade to open the lumen side of hollow fibers. Polyvinyl chloride connectors with reducing unions were glued to each end with Tangit adhesive. The active length of ME was 0.48 m, the potted length was 0.05 m, the active membrane area was 2.75 m^2, and the packing density was 53%.

The shell side of the membrane element was treated with 1% wt. PDMS solution in hexane. After draining the solution, the ME was vented with air for 24 h and annealed at 60 °C in the air for 24 h. Fibers were treated with silicone after potting because it was found that PDMS-coating reduced the adhesion of fibers to polyurea potting resin. This resulted in the decrease of separation selectivity due to partial non-selective flow through the regions between fibers and potting material, where the adhesion was insufficient. Moreover, PDMS treatment after potting plugged pinholes in fibers which could be formed during the handling, centrifugation, or polyurea resin setting.

2.4. Membrane Element's Pure and Mixed Gas Test

The pure gas permeation experiments were executed in the same setup as for individual hollow fibers with the closed retentate outlet port to determine pure gas permeances of nitrogen and oxygen.

In mixed gas tests, atmospheric air was compressed and fed to the ME at a certain pressure. The residue flow rate was controlled by a needle flow regulator on the outlet of ME. The flow rate of feed, retentate (residue, non-permeated gas stream), and permeate (permeated gas stream) was determined using SMC flow meters (Japan). The permeate stream exited the ME at atmospheric pressure. The tests were conducted under isothermal conditions at ambient temperature (22 ± 2 °C). The oxygen concentration of permeate and retentate was measured using O_2 gas analyzer (LLC AnalitTeploKontrol, Smolensk, Russia).

To calculate the permeance and selectivity, counter-current mathematical model was employed, which involved the solution of the system of two differential linear equations using Euler's method. The algorithm is described elsewhere [28,29].

3. Results and Discussion

3.1. Hollow Fiber Spinning and Characterization

Determination of the gas permeance and selectivity values is a widely used technique to judge the selective layer thickness and the presence of defects. For dense polysulfone membranes, the permeability of O_2 is 1.06–1.18 Barrer and the O_2/N_2 selectivity is 5.8–6.2 at 25 °C [19,30]. According to Knudsen diffusion, oxygen/nitrogen selectivity is equal to the square root of the inverse ratio of their molecular weights: $\alpha_{KN}(O_2/N_2) = 0.935$. According to the Hagen–Poiseuille model, the ratio of oxygen to nitrogen permeance is equal to the inverse ratio of gas viscosities, approximately 0.867.

From Table 1, it can be noticed that all of the hollow fibers have pin-holes in the skin layer because the selectivity is less than polysulfone intrinsic value. For the dope temperature 62 °C (sample #1), an increase in the take-up speed from 30 to 45 m/min (sample #2) or reduction in the air gap height (sample #3) resulted in the rise of permeance and a decline of the selectivity. This was connected with the decrease of the selective layer thickness and occurred due to the decline of the time spent in the air gap, where volatile THF readily evaporates [22]. Permeance and selectivity values show that the transport mechanism is transitional between the Knudsen and solution-diffusion models.

After treatment with PDMS, the intrinsic value of PSf selectivity was attained, suggesting that all defects were plugged. The effective skin-layer thickness derived from oxygen permeance was 66 nm.

Table 1. The influence of spinning parameters on hollow fibers' geometrical and gas separation characteristics before and after polydimethylsiloxane (PDMS) treatment.

#	T [1], °C	Air Gap, cm	υ [2], m/min	OD, μm	ID, μm	P/l(O_2) [3]	α(O_2/N_2)	P/l(O_2) [3,4]	α(O_2/N_2) [4]	l [5], nm
1	62	20	30	215	140	55	3.1	45	5.9	66
2	62	20	45	190	115	164	1.6	45	6.1	66
3	62	10	30	215	140	79	2.1	41	6.0	72
4	25	10	30	235	160	1122	1.0	265	1.8	-
5	25	20	30	230	155	450	1.1	70	6.0	42
6	25	25	30	225	150	284	1.4	59	6.1	50

[1] T-dope temperature; [2] υ-take-up speed; [3] P/l-permeance in L (STP)/(m^2·h·bar); [4] after PDMS treatment; [5] effective selective layer thickness of the PDMS-treated sample calculated from oxygen permeance

The decrease in the dope solution temperature to 25 °C reduced the rate of THF evaporation in the air gap, which resulted in the decline of the selectivity and raised the permeance. Gas separation characteristics of sample #4 indicated the highest surface porosity and a transport mechanism shifting towards the Hagen–Poiseuille model. All of the surface pores were not covered with a PDMS layer in a single application.

Sample #5 possessed the highest permeance after PDMS treatment and intrinsic PSf selectivity. The effective skin-layer thickness derived from oxygen permeance was 42 nm, which was consistent with the results of the previous studies [17,19].

It is worth noting that the permeability of PDMS is two orders of magnitude higher than that of PSf, and consequently, PDMS brings a negligible resistance to the mass transfer through the fiber wall when applied as a thin layer [5]. The resistance increases when a high permeable polymer penetrates into the pores of the support [5,14]. Permeance and selectivity of the untreated sample #1 suggested that the size and the number of defects on the top-surface were too small for the solution of silicone to enter the pores. In such conditions, a thin layer of PDMS was formed, which negligibly declined the permeance of sample #1 compared to other samples where the penetration of silicone into the pores was notable.

Macrovoids with length up to 19 μm and width up to 6 μm were observed in the cross-section of the sample #1 (Figure 4a) at the lumen side of the fiber. Macrovoids with length up to 30 μm and width up to 13 μm were observed in the cross-section of the sample #2 (Figure 4b). The cross-section of sample #5 (Figure 4c) had a different microstructure and displayed the absence of macrovoids. The SEM micrograph of the sample #5 selective layer region (Figure 4d) showed a layer with the thickness up to 2 μm, composed of a dense separating layer supported by a structure containing numerous micropores and channels.

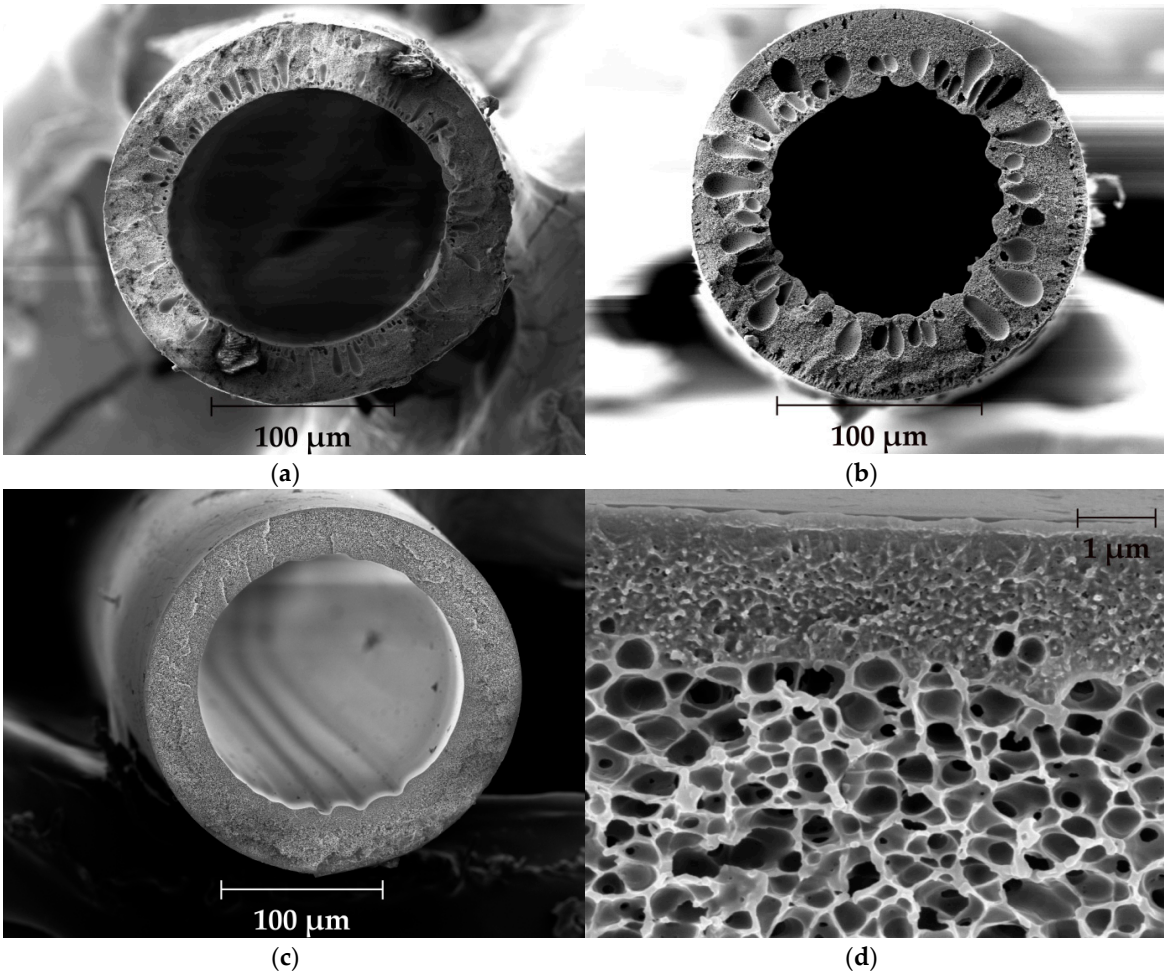

Figure 4. SEM micrographs of hollow fiber: (**a**) Sample #1, cross-section; (**b**) Sample #2, cross-section; (**c**) Sample #5, cross-section; (**d**) Sample #5, cross-section with the zoom of the selective layer.

The generation of macrovoids on the lumen side of the fiber occurs during nonsolvent-induced phase separation. Upon the contact of the dope solution with the internal coagulant (water), fast exchange of solvent and non-solvent takes places through the interfacial layer. Nucleation of the polymer lean phase can start below this layer, caused by the diffusionally controlled movement of the precipitation front through the hollow fiber wall [31]. Nuclei can expand isotropically from the time of their initiation unless the stiffness of the nucleus wall resists the diffusive driving forces for their growth. Macrovoids appear if the inward diffusion rate of water greatly exceeds the rate of outward solvent diffusion from the nucleus [32]. Apparently, this was the reason for macrovoid formation, taking into account the large difference between the diffusion coefficients of water and larger organic molecules: DMAc and THF. Moreover, the diffusion influx of the solvent from the dope into the nucleus through the plasticized "front side" is greater than the outflow of solvent from the nucleus through the vitrified "backside". Such ingress of the solvent must be responsible for the size and teardrop shape of the observed macrovoids [32].

Apparently, the decrease in the dope temperature allowed to diminish macrovoids due to the increase of the dope viscosity from 15.5 Pa·s at 62 °C to 35 Pa·s at 25 °C. With the reduction in the dope viscosity, the "front side" of the nucleus starts to experience resistance which impedes its expansion, and the solvent diffusivity into the nucleus decreases. In these conditions, the macrovoid growth rate slows down and equalizes with the velocity of the precipitation front, the nucleus seizes expansion and new nucleus forms in front.

The comparison of literature data devoted to the development of PSf hollow fibers for gas separation with the results obtained in this work is presented in Table 2. The fibers produced in the current work have similar gas separation characteristics as in [19] and [21], but have a macrovoid free structure, unlike [19]. In work [21], the dope solution contained 37% wt. of the polymer, and its viscosity was >100 Pa·s at 70 °C. In practice, it is hard to prepare, degas, and spin dopes with such a high value of viscosity. Moreover, the propionic acid which was used in [21] as a non-solvent has a pungent and unpleasant smell. This fact complicates the spinning process, especially at high dope temperature.

Table 2. The comparison of obtained results with the literature data.

Work	P/l (O_2) [1]	$\alpha(O_2/N_2)$	l, nm	T, Δp [2]	Macrovoids
[17]	-	-	400	25 °C, 8 bar	+
[19]	55–80	5–6.5	36–50	25 °C, 5 bar	+
[20]	-	-	500–700	50 °C	–
[21]	116	5–5.2	-	50 °C, 13.6 bar	–
This work	70	6.0	42	22 °C, 5 bar	–

[1] in L (STP)/(m^2·h·bar); [2] experimental conditions of gas permeance measurement.

3.2. Membrane Element Characterization

The membrane element was obtained using a batch of sample #5 fibers and was tested in the process of air separation. The pure oxygen permeance of this ME was 80 L (STP)/(m^2·h·bar), and the selectivity was 5.5, which is in good agreement with the results obtained for the individual fibers (Table 1).

As expected, an increase in the product purity (nitrogen concentration in the retentate) grew the stage cut–a dimensionless ratio of permeate to feed-gas flow rates (Table 3). At the same time, the calculated selectivity decreased and was significantly lower than the value measured by pure gases. The reason for such behavior is that at a given concentration of nitrogen, the stage cut was higher than it was expected from pure gas permeance. Such deviations could be caused by several factors.

Table 3. The relation of product (nitrogen) purity with the separation characteristics of the hollow fiber membrane element.

ΔP, bar	x_r,%	q_r, m^3/h	q_p, m^3/h	θ	P/l (O_2) [1]	$\alpha(O_2/N_2)$
5	6.2	0.29	0.36	0.55	74.4	4.1
5	4.8	0.21	0.33	0.61	74.2	4.0
5	0.9	0.06	0.31	0.83	81.1	3.6
7	4.9	0.4	0.53	0.57	87.6	4.2

[1] in L (STP)/(m^2·h·bar); x_r – oxygen concentration in the retentate, q_r and q_p – retentate and permeate flow rates.

Firstly, it was shown that variations in fiber diameter, permeance, and selectivity within one ME could deteriorate the performance of the ME [3,33]. Secondly, the concentration polarization in the porous support is of major concern for the bore-side feed configuration. Deviations, caused by these reasons, increase especially for high retentate concentrations [1,3], which agrees well with the observed data.

With an increase in the transmembrane pressure, the gas separation characteristics slightly improved. This effect was observed in work [4] and was ascribed to pressure-induced deformations in the separating layer, especially enlargements of the rubber parts of polymer.

4. Conclusions

Spinning parameters to obtain high permeable and defect free polysulfone hollow fibers for gas separation are shown in this work. It was demonstrated that fibers with the initial selectivity close to unity could be used for this purpose if proper PDMS treatment is conducted. Using this

approach, the hollow fibers with the effective skin-layer thickness of 42 nm were derived. It was found that macrovoids could be completely eliminated by reducing the dope viscosity without any deterioration in gas separation characteristics. From approximately 8000 fibers, a membrane element with an active membrane area of 2.75 m^2 was assembled, which is on the state-of-the-art level of commercial membrane elements. This membrane element allowed to produce nitrogen with purity >99%. Its individual gas permeance is in good agreement with the results obtained for the individual fibers. Apparently, due to variations in fiber diameter, permeance, and selectivity within one ME and concentration polarization, the calculated selectivity was lower than the value measured by pure gases.

Author Contributions: Conceptualization, investigation, methodology, Writing—Original Draft, review, and editing, G.D.; Investigation and methodology, M.I., M.S., V.S., and N.F.; Supervision, G.K.

Funding: This research received no external funding.

Conflicts of Interest: The authors declare no conflict of interest.

References

1. Feng, X.; Ivory, J.; Rajan, V.S.V. Air separation by integrally asymmetric hollow-fiber membranes. *AIChE J.* **1999**, *45*, 2142–2152. [CrossRef]
2. Dibrov, G.; Ivanov, M.; Semyashkin, M.; Sudin, V.; Kagramanov, G. High-Pressure Aging of Asymmetric Torlon® Hollow Fibers for Helium Separation from Natural Gas. *Fibers* **2018**, *6*, 83. [CrossRef]
3. Rautenbach, R.; Struck, A.; Roks, M.F.M. A variation in fiber properties affects the performance of defect-free hollow fiber membrane modules for air separation. *J. Membr. Sci.* **1998**, *150*, 31–41. [CrossRef]
4. Rautenbach, R.; Struck, A.; Melin, T.; Roks, M.F.M. Impact of operating pressure on the permeance of hollow fiber gas separation membranes. *J. Membr. Sci.* **1998**, *146*, 217–223. [CrossRef]
5. Henis, J.M.S.; Tripodi, M.K. Composite Hollow Fiber Membranes for Gas Separation: The Resistance Model Approach. *J. Membr. Sci.* **1981**, *8*, 233–246. [CrossRef]
6. Bildyukevich, A.V.; Plisko, T.V.; Liubimova, A.S.; Volkov, V.V.; Usosky, V.V. Hydrophilization of polysulfone hollow fiber membranes via addition of polyvinylpyrrolidone to the bore fluid. *J. Membr. Sci.* **2017**, *524*, 537–549. [CrossRef]
7. Bildyukevich, A.V.; Usosky, V.V. Prevention of the capillary contraction of polysulfone based hollow fiber membranes. *Pet. Chem.* **2014**, *54*, 652–658. [CrossRef]
8. Plisko, T.V.; Bildyukevich, A.V.; Usosky, V.V.; Volkov, V.V. Influence of the concentration and molecular weight of polyethylene glycol on the structure and permeability of polysulfone hollow fiber membranes. *Pet. Chem.* **2016**, *56*, 321–329. [CrossRef]
9. Bildyukevich, A.V.; Plisko, T.V.; Usosky, V.V. The formation of polysulfone hollow fiber membranes by the free fall spinning method. *Pet. Chem.* **2016**, *56*, 379–400. [CrossRef]
10. Kostyanaya, M.; Bazhenov, S.; Borisov, I.; Plisko, T.; Vasilevsky, V. Surface Modified Polysulfone Hollow Fiber Membranes for Ethane/Ethylene Separation Using Gas-Liquid Membrane Contactors with Ionic Liquid-Based Absorbent. *Fibers* **2019**, *7*, 4. [CrossRef]
11. Kirsch, V.A.; Bildyukevich, A.V.; Bazhenov, S.D. Simulation of Convection–Diffusion Transport in a Laminar Flow Past a Row of Parallel Absorbing Fibers. *Fibers* **2018**, *6*, 90. [CrossRef]
12. Bazhenov, S.D.; Bildyukevich, A.V.; Volkov, A.V. Gas-Liquid Hollow Fiber Membrane Contactors for Different Applications. *Fibers* **2018**, *6*, 76. [CrossRef]
13. Borisov, I.; Ovcharova, A.; Bakhtin, D.; Bazhenov, S.; Volkov, A.; Ibragimov, R.; Gallyamov, R.; Bondarenko, G.; Mozhchil, R.; Bildyukevich, A.; et al. Development of Polysulfone Hollow Fiber Porous Supports for High Flux Composite Membranes: Air Plasma and Piranha Etching. *Fibers* **2017**, *5*, 6. [CrossRef]
14. Volkov, V.V.; Bildukevich, A.V.; Dibrov, G.A.; Usoskiy, V.V.; Kasperchik, V.P.; Vasilevsk, V.P.; Novitsky, E.G. Elaboration of Composite Hollow Fiber Membranes with Selective Layer from Poly [1-(trimethylsylil). 1-propyne] for Regeneration of Aqueous Alkanolamine Solutions. *Pet. Chem.* **2013**, *53*, 619–626. [CrossRef]
15. Ovcharova, A.; Vasilevsky, V.; Borisov, I.; Bazhenov, S.; Volkov, A.; Bildyukevich, A.; Volkov, V. Polysulfone porous hollow fiber membranes for ethylene-ethane separation in gas-liquid membrane contactor. *Sep. Purif. Technol.* **2017**, *183*, 162–172. [CrossRef]

16. Malakhov, A.O.; Bazhenov, S.D.; Vasilevsky, V.P.; Borisov, I.L.; Ovcharova, A.A.; Bildyukevich, A.V.; Volkov, V.V.; Giorno, L.; Volkov, A.V. Thin-film composite hollow fiber membranes for ethylene/ethane separation in gas-liquid membrane contactor. *Sep. Purif. Technol.* **2019**, *219*, 64–73. [CrossRef]
17. Aroon, M.A.; Ismail, A.F.; Montazer-Rahmati, M.M.; Matsuura, T. Morphology and permeation properties of polysulfone membranes for gas separation: Effects of non-solvent additives and co-solvent. *Sep. Purif. Technol.* **2010**, *72*, 194–202. [CrossRef]
18. Tsai, H.A.; Kuo, C.Y.; Lin, J.H.; Wang, D.M.; Deratani, A.; Pochat-Bohatier, C.; Lee, K.R.; Lai, J.Y. Morphology control of polysulfone hollow fiber membranes via water vapor induced phase separation. *J. Membr. Sci.* **2006**, *278*, 390–400. [CrossRef]
19. Wang, D.; Teo, W.K.; Li, K. Preparation and characterization of high-flux polysulfone hollow fibre gas separation membranes. *J. Membr. Sci.* **2002**, *204*, 247–256. [CrossRef]
20. Fritzsche, A.K. Asymmetric Polysulfone Hollow Fiber Membranes for Gas Separations. In *Applications of Polymers*; Seymour, R.B., Mark, H.F., Eds.; Springer: Boston, MA, USA, 1988.
21. Kesting, R.E.; Fritzsche, A.K.; Murphy, M.K.; Cruse, C.A.; Handermann, A.C.; Malon, R.F.; Moore, M.D. The second-generation polysulfone gas-separation membrane. I. The use of lewis acid: Base complexes as transient templates to increase free volume. *J. Appl. Polym. Sci.* **1990**, *40*, 1557–1574. [CrossRef]
22. Ivanov, M.V.; Storozhuk, I.P.; Dibrov, G.A.; Semyashkin, M.P.; Pavlukovich, N.G.; Kagramanov, G.G. Elaboration of hollow fiber membrane from polyarylate-polyarylate block-copolymer for air separation. *Pet. Chem.* **2018**, *8*, 85–92.
23. Ivanov, M.V.; Dibrov, G.A.; Loyko, A.V.; Varezhkin, A.V.; Kagramanov, G.G. Techniques to Manage Geometry Characteristics of Hollow Fiber Membranes. *Theor. Found. Chem. Eng.* **2016**, *50*, 316–324. [CrossRef]
24. Roy, S.; Singha, N.R. Polymeric Nanocomposite Membranes for Next Generation Pervaporation Process: Strategies, Challenges and Future Prospects. *Membranes* **2017**, *7*, 53. [CrossRef]
25. Grushevenko, E.A.; Borisov, I.L.; Bakhtin, D.S.; Legkov, S.A.; Bondarenko, G.N.; Volkov, A.V. Membrane material based on octyl-substituted polymethylsiloxane for separation of C3/C1 hydrocarbons. *Pet. Chem.* **2017**, *57*, 334–340. [CrossRef]
26. Grushevenko, E.A.; Borisov, I.L.; Bakhtin, D.S.; Bondarenko, G.N.; Levin, I.S.; Volkov, A.V. Silicone rubbers with alkyl side groups for C3+ hydrocarbon separation. *React. Funct. Polym.* **2019**, *134*, 156–165. [CrossRef]
27. Dibrov, G.A.; Volkov, V.V.; Vasilevsky, V.P.; Shutova, A.A.; Bazhenov, S.D.; Khotimsky, V.S.; van de Runstraat, A.; Goetheer, E.L.V.; Volkov, A.V. Robust high-permeance PTMSP composite membranes for CO_2 membrane gas desorption at elevated temperatures and pressure. *J. Membr. Sci.* **2014**, *470*, 439–450. [CrossRef]
28. Pan, C.Y. Gas Separation by Permeators with High-Flux Asymmetric Membranes. *AIChE J.* **1983**, *29*, 545–552. [CrossRef]
29. Davis, R.; Sandall, O. A Simple Analysis for Gas Separation Membrane Experiments. *Chem. Eng. Educ.* **2003**, *37*, 74–80.
30. Nagase, Y.; Naruse, A.; Matsui, K. Chemical modification of polysulphone: 2. Gas and liquid permeability of polysulphone/polydimethylsiloxane graft copolymer membranes. *Polymer* **1990**, *31*, 121–125. [CrossRef]
31. Smolders, C.A.; Reuvers, A.J.; Boom, R.M.; Wienk, I.M. Microstructures in phase-inversion membranes. Part 1. Formation of macrovoids. *J. Membr. Sci.* **1992**, *73*, 259–275. [CrossRef]
32. McKelvey, S.A.; Koros, W.J. Phase separation, vitrification, and the manifestation of macrovoids in polymeric asymmetric membranes. *J. Membr. Sci.* **1996**, *112*, 29–39. [CrossRef]
33. Lemanski, J.; Lipscomb, G.G. Effect of fiber variation on the performance of countercurrent hollow fiber gas separation modules. *J. Membr. Sci.* **2000**, *167*, 241–252. [CrossRef]